# Electronic Supplementary Information

## Dual-emitting Tb(III)&Yb(III) functionalized coordination polymer: "turn-on" sensor for N-methylformamide in urine and "turn-off" sensor for methylglyoxal in serum

Xubin Zheng,[a] Ruiqing Fan,[*a] Haoyang Lu,[a] Bowen Wang,[a] Jingkun Wu,[a] Ping Wang[a] and Yulin Yang[*a]

[a]MIIT *Key Laboratory of Critical Materials Technology for New Energy Conversion and Storage, School of Chemistry and Chemical Engineering, Harbin Institute of Technology, Harbin 150001, P. R. of China*

*Corresponding Author: Ruiqing Fan and Yulin Yang

**E-mail:** fanruiqing@hit.edu.cn and ylyang@hit.edu.cn

## Experimental Section

### Materials and methods

All chemicals employed were commercially available reagents of analytical grade and used without further purification. 1-(4-carboxylbenzyl)-3-(pyrzin-2-yl) (97%, Hcbpp) was purchased from Jinan Henghua Sci .& Tec .Co.,Ltd. Elemental analyses were carried out on a Perkin–Elmer 2400 automatic analyzer. FT–IR spectra data (4000–400 $cm^{-1}$) were collected by a Nicolet impact 410 FT–IR spectrometer. The emission properties were recorded with Edinburgh FLS 920 fluorescence spectrometer equipped with a Peltier-cooled Hamamatsu R928 photomultiplier tube. An Edinburgh Xe900 450 W xenon arc lamp was used as an exciting light source. Thermal analysis was performed on a ZRY-2P thermogravimetric analysis from 30 to 700 °C with a heating rate of 10 °C $min^{-1}$ under a flow of air. Powder X-ray diffraction (PXRD) patterns were recorded in the 2θ range of 5 – 50° using Cu Kα radiation with a Shimadzu XRD-6000 X-ray diffractometer. Elemental analyses for Cu and Tb were conducted using a Perkin-Elmer Model Optima 3300 DV ICP spectrometer. Density functional theory (DFT) calculations were conducted by using the B3LYP/lanl2dz basis set implemented in the Gaussian 09 package. XPS experiments were carried out on a RBD upgraded PHI-5000C ESCA system (Perkin Elmer) with Mg Kα radiation (hν = 1253.6 eV). Lifetime studies were performed using photon-counting system with a microsecond pulse lamp as the excitation source. Data were analyzed through the nonlinear least squares procedure in combination with an iterative convolution method. The emission decays were analyzed by the sum of exponential functions. The decay curve is well fitted into a double exponential function: $I = I_0 + A_1 \exp(-t/\tau_1) + A_2 \exp(-t/\tau_2)$, where $I$ and $I_0$ are the luminescent intensities at time $t = t$ and $t = 0$, respectively, whereas $\tau_1$ and $\tau_2$ are defined as the luminescent lifetimes. The average lifetime was calculated according to the following equation: $\frac{\tau_1^2 A_1\% + \tau_2^2 A_2\%}{\tau_1 A_1\% + \tau_2 A_2\%}$.

**X-ray data collection and structure determinations**

X-ray single-crystal diffraction data of Cu-cbpp and Cu-Hcbpp were collected on a Rigaku SCX-mini diffractometer with graphite monochromatic Mo-Kα radiation (λ = 0.71073 Å). The program CrystalClear was used for integration of the diffraction profiles. All the structures were solved by direct methods using the SHELXS program of the SHELXTL package and refined by full-matrix least-squares methods with SHELXL. Metal atoms were located from the E-maps and other non-hydrogen atoms excluded in conterions were located in successive difference Fourier syntheses and refined with anisotropic thermal parameters on $F^2$. Further details of crystal data and structure refinement for Cu-cbpp and Cu-Hcbpp were summarized in Table S1.

**Table S1** Crystal data and structure refinement parameters

| Identification code | Cu-cbpp | Cu-Hcbpp |
|---|---|---|
| Empirical formula | $C_{30}H_{22}Cl_2Cu_2N_8O_4$ | $C_{30}H_{24}Cl_4Cu_2N_8O_4$ |
| CCDC | 1920117 | 1920118 |
| Formula mass | 756.54 | 829.47 |
| Crystal system | Monoclinic | Triclinic |
| Space group | $P\,2_1/c$ | $P$ |
| $a$ (Å) | 7.213(6) | 7.305(9) |
| $b$ (Å) | 12.897(11) | 8.862(11) |
| $c$ (Å) | 15.843(13) | 24.838(3) |
| $\alpha$ (˚) | 90.00 | 92.59(2) |
| $\beta$ (˚) | 95.39(10) | 97.87(2) |
| $\gamma$ (˚) | 90.00 | 96.67(2) |
| V (Å$^3$) | 1467.3(2) | 1578.8(3) |
| Z | 2 | 2 |
| $D_c$/(g cm$^{-3}$) | 1.712 | 1.745 |
| $\mu$ (Mo Kα)/mm$^{-1}$ | 1.685 | 1.738 |
| $F$(000) | 764 | 836 |
| $\theta$ range (°) | 2.58 – 27.65 | 0.83 – 25.00 |
| Limiting indices | $-8 \le h \le 9$ | $-8 \le h \le 8$ |
| | $-15 \le k \le 16$ | $-9 \le k \le 10$ |
| | $-18 \le l \le 20$ | $-29 \le l \le 29$ |
| Data/Restraints/Parameters | 3365 / 0 / 208 | 5550 / 0 / 433 |
| GOF on $F^2$ | 1.038 | 1.056 |
| $R_1$[a] | 0.0322 | 0.0373 |
| $wR_2$[b] | 0.0812 | 0.0913 |
| $R_1$ | 0.0434 | 0.0580 |
| $wR_2$ | 0.0865 | 0.1113 |

[a] $R_1 = \sum||F_o| - |F_c||/\sum|F_o|$;

[b] $wR_2 = [\sum[\, w\,(F_o^2 - F_c^2)^2] / \sum[\, w\,(F_o^2)^2]]^{1/2}$.

**Table S2** Selected bond lengths (Å) and bond angles (°)

| | | | |
|---|---|---|---|
| Cu-cbpp | | | |
| Cu(1)-N(2) | 2.006(18) | N(2)-Cu(1)-O(2) | 162.18(7) |
| Cu(1)-O(2) | 2.010(17) | N(2)-Cu(1)-O(1) | 97.86(7) |
| Cu(1)-O(1) | 2.046(17) | O(2)-Cu(1)-O(1) | 64.60(7) |
| Cu(1)-N(3) | 2.176(18) | N(2)-Cu(1)-N(3) | 78.56(7) |
| Cu(1)-Cl(1) | 2.228(7) | O(2)-Cu(1)-N(3) | 101.04(7) |
| | | O(1)-Cu(1)-N(3) | 101.69(7) |
| | | N(2)-Cu(1)-Cl(1) | 96.58(6) |
| | | O(2)-Cu(1)-Cl(1) | 99.68(5) |
| | | O(1)-Cu(1)-Cl(1) | 143.01(6) |
| | | | |
| Cu-Hcbpp | | | |
| Cu(1)-N(1) | 2.046(3) | N(3)-Cu(1)-Cl(1) | 170.32(9) |
| Cu(1)-N(3) | 2.065(3) | Cl(2)-Cu(1)-Cl(1) | 92.18(4) |
| Cu(1)-Cl(2) | 2.2371(10) | N(1)-Cu(1)-Cl(4) | 99.03(9) |
| Cu(1)-Cl(1) | 2.2716(10) | N(3)-Cu(1)-Cl(4) | 89.51(9) |
| Cu(1)-Cl(4) | 2.8791(12) | Cl(2)-Cu(1)-Cl(4) | 96.06(4) |
| Cu(2)-N(5) | 2.047(3) | Cl(1)-Cu(1)-Cl(4) | 89.12(4) |
| Cu(2)-N(7) | 2.076(3) | N(5)-Cu(2)-N(7) | 79.81(12) |
| Cu(2)-Cl(4) | 2.2526(11) | N(5)-Cu(2)-Cl(4) | 175.14(9) |
| Cu(2)-Cl(3) | 2.2586(10) | N(7)-Cu(2)-Cl(4) | 97.83(9) |
| Cu(2)-Cl(1) | 2.9330(12) | N(5)-Cu(2)-Cl(3) | 90.86(9) |
| | | N(7)-Cu(2)-Cl(3) | 168.59(9) |
| | | Cl(4)-Cu(2)-Cl(3) | 91.94(4) |
| N(1)-Cu(1)-N(3) | 79.84(12) | N(5)-Cu(2)-Cl(1) | 87.38(9) |
| N(1)-Cu(1)-Cl(2) | 164.64(9) | N(7)-Cu(2)-Cl(1) | 83.75(8) |
| N(3)-Cu(1)-Cl(2) | 97.49(9) | Cl(4)-Cu(2)-Cl(1) | 88.14(4) |
| N(1)-Cu(1)-Cl(1) | 90.92(9) | Cl(3)-Cu(2)-Cl(1) | 102.52(4) |

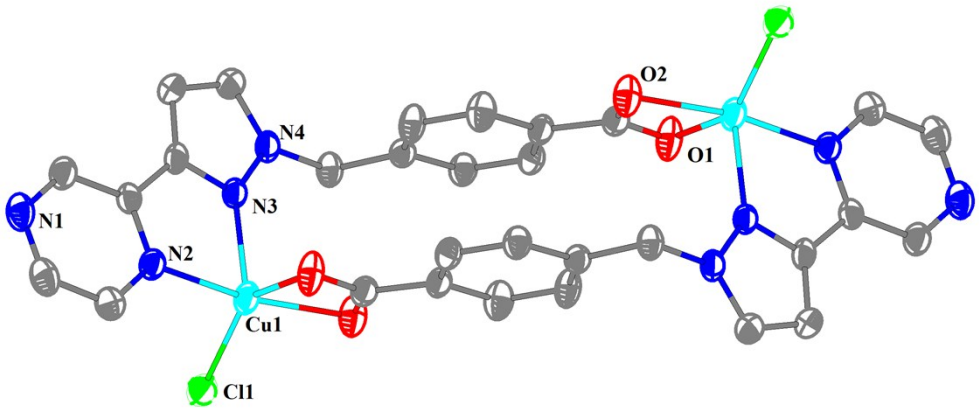


**Fig. S1** The structural unit of Cu-cbpp with labeling scheme and 50% thermal ellipsoids (hydrogen atoms are omitted for clarity)

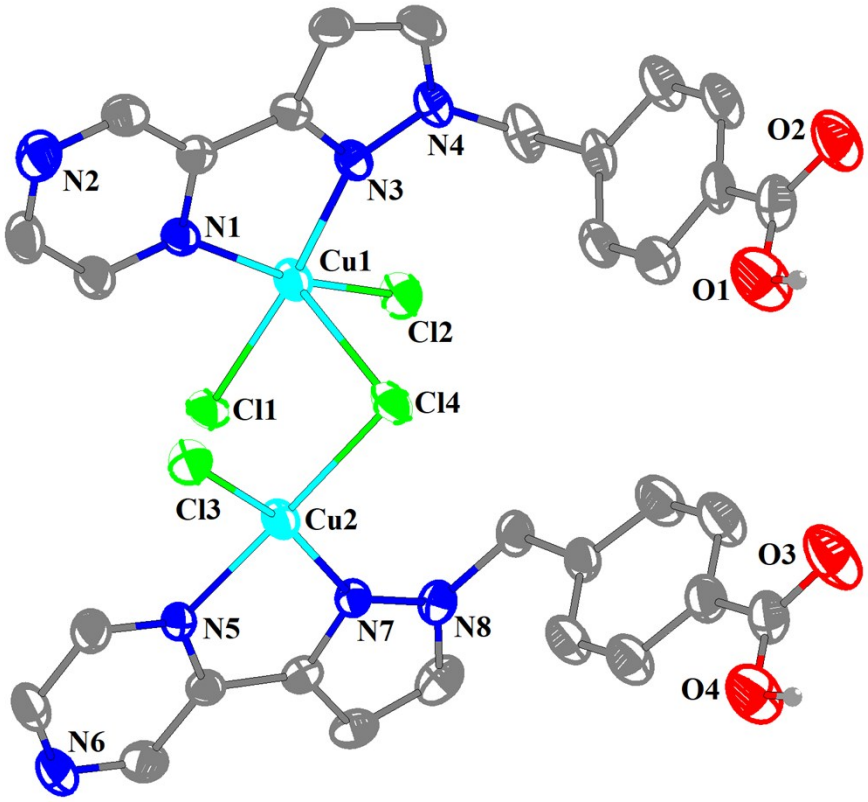


**Fig. S2** The structural unit of Cu-Hcbpp with labeling scheme and 50% thermal ellipsoids (hydrogen atoms are omitted for clarity)

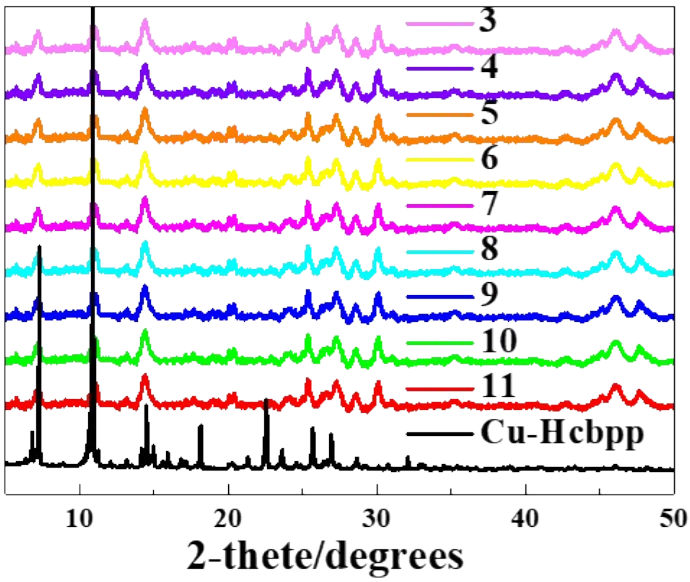


**Fig. S3** PXRD patterns of Tb@Cu-Hcbpp in different pH value (from 3 to 11)

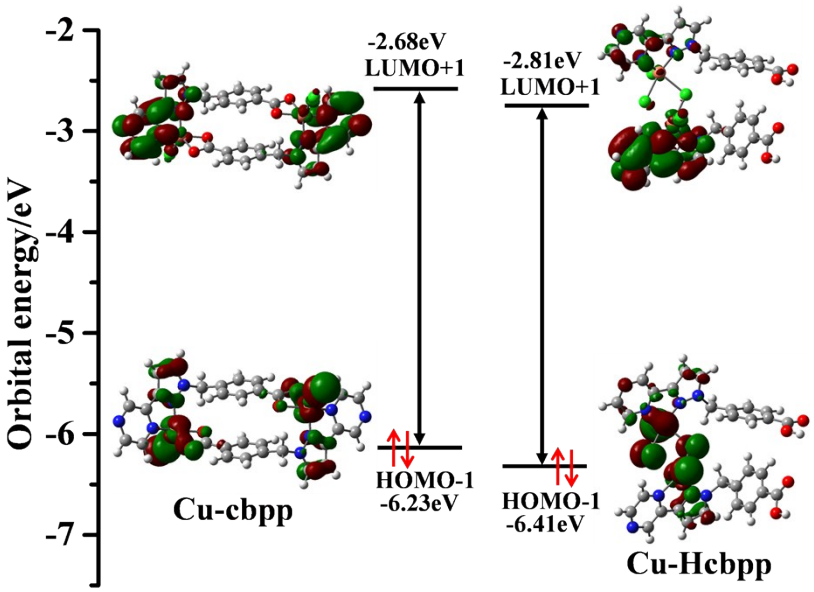


**Fig. S4** Electron distribution and energy diagram of HOMO-1 and LUMO+1 orbitals for Cu-cbpp and Cu-Hcbpp.

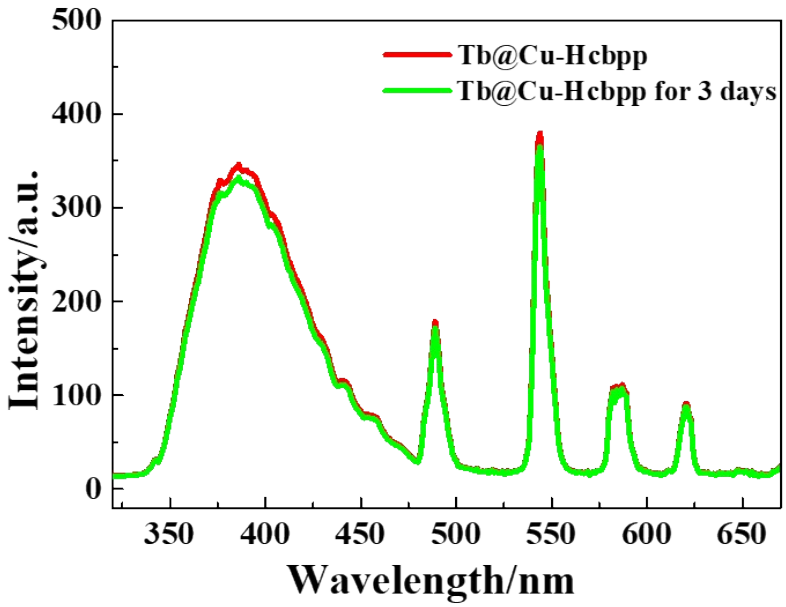


**Fig. S5** Fluorescence spectra of Tb@Cu-Hcbpp for 3 days

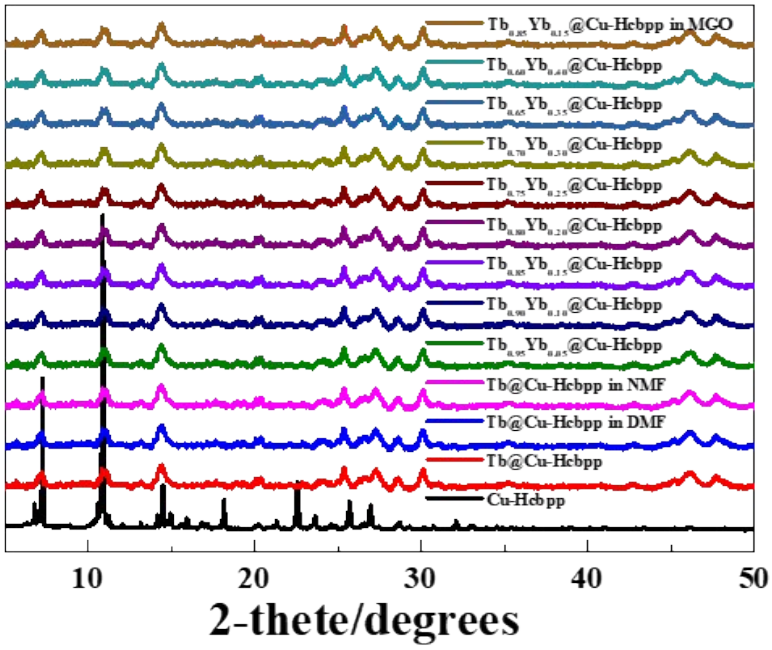


**Fig. S6** PXRD patterns of Tb@Cu-Hcbpp in different conditions

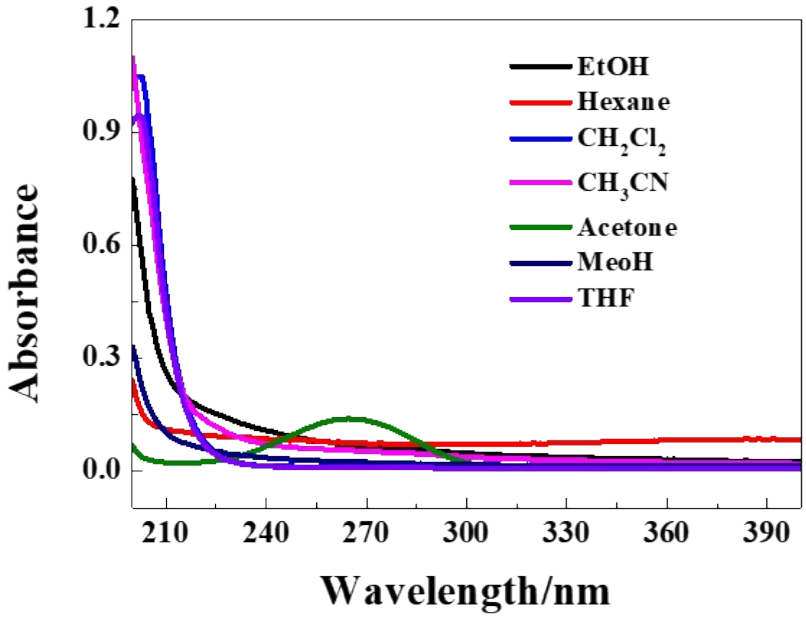


**Fig. S7** UV-vis spectra of various organic solvents

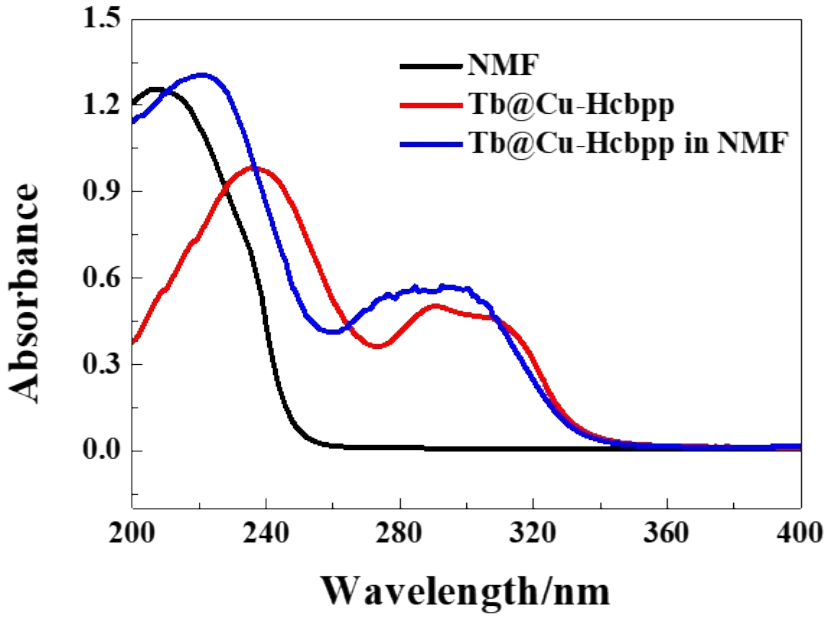


**Fig. S8** UV-vis spectra of Tb@Cu-Hcbpp in related circumstances

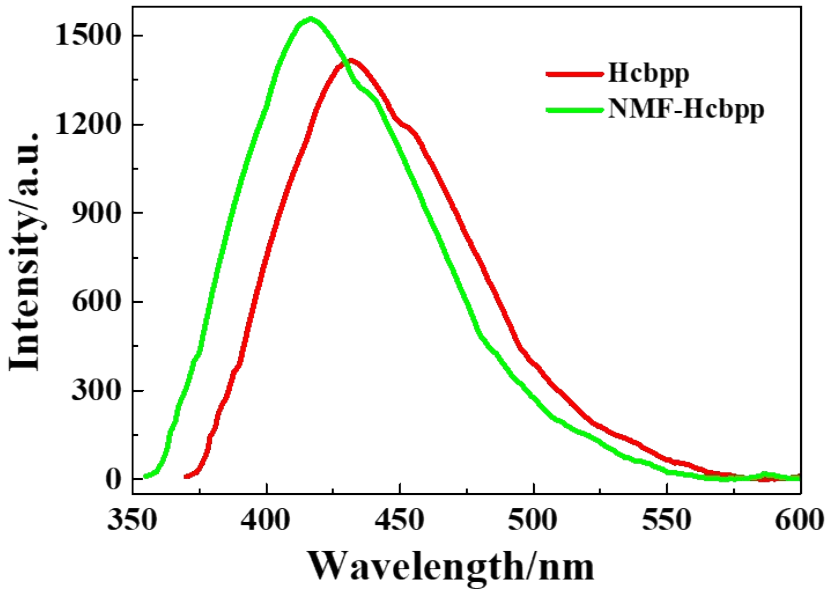


**Fig. S9** Fluorescence response of Hcbpp in NMF

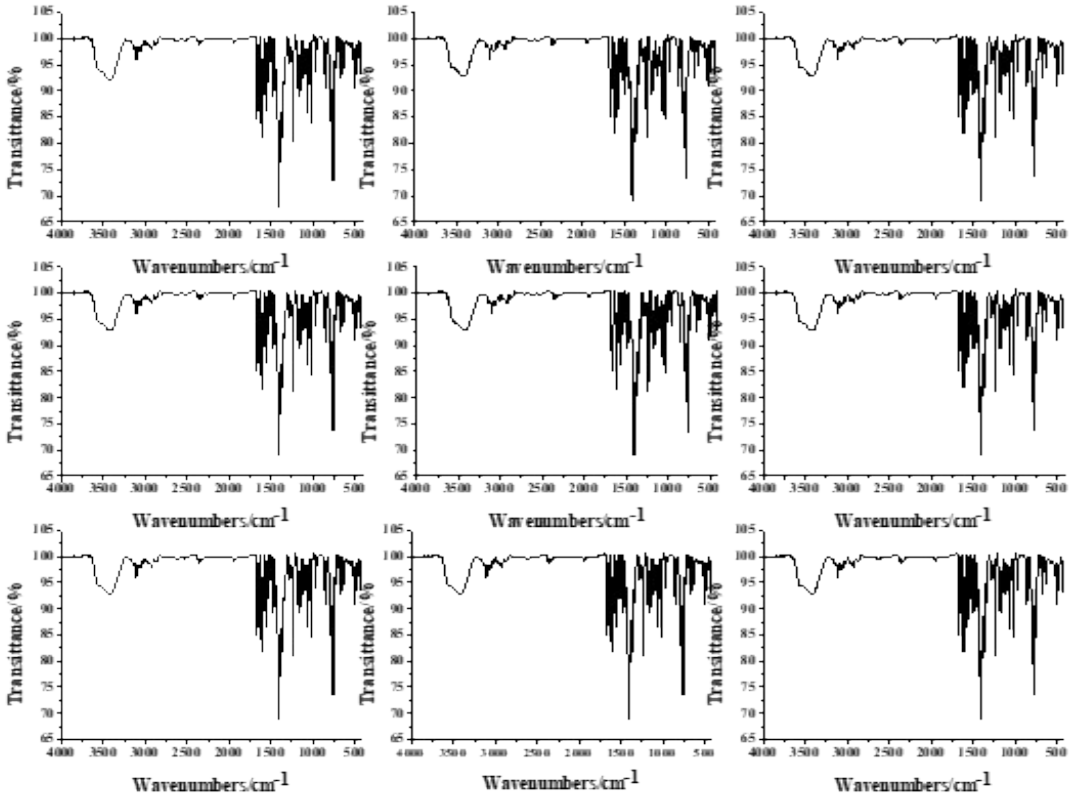


**Fig. S10** FT-IR spectra of $Tb_{1-x}Yb_x$@Cu-Hcbpp (x =0, 0.05, 0.10, 0.15, 0.20, 0.25, 0.30, 0.35 and 0.40)

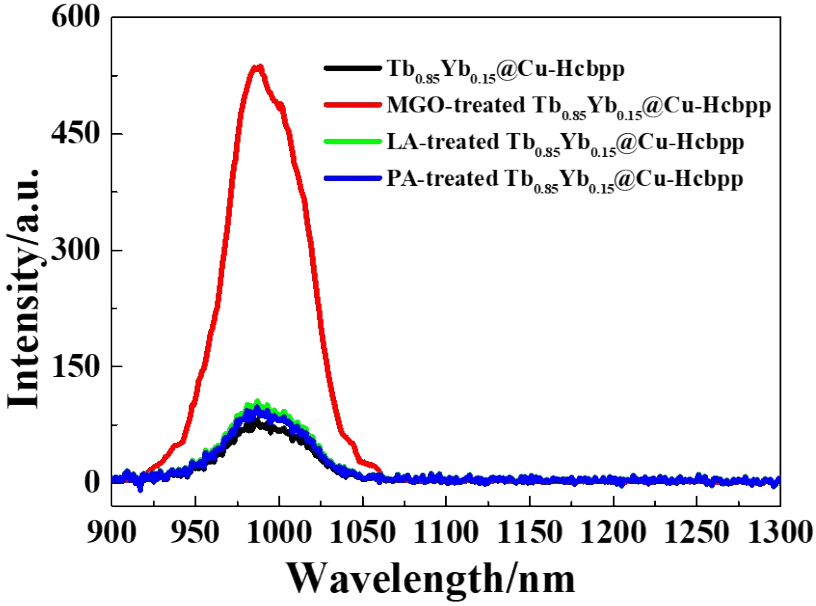


**Fig. S11** $Yb^{3+}$ ions emission of $Tb_{0.85}Yb_{0.15}$@Cu-Hcbpp with MGO, LA or PA.

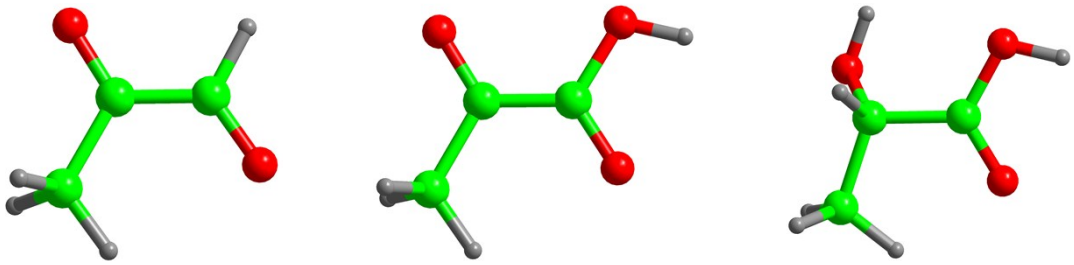


**Fig. S12** The molecular structure of MGO, PA and LA.

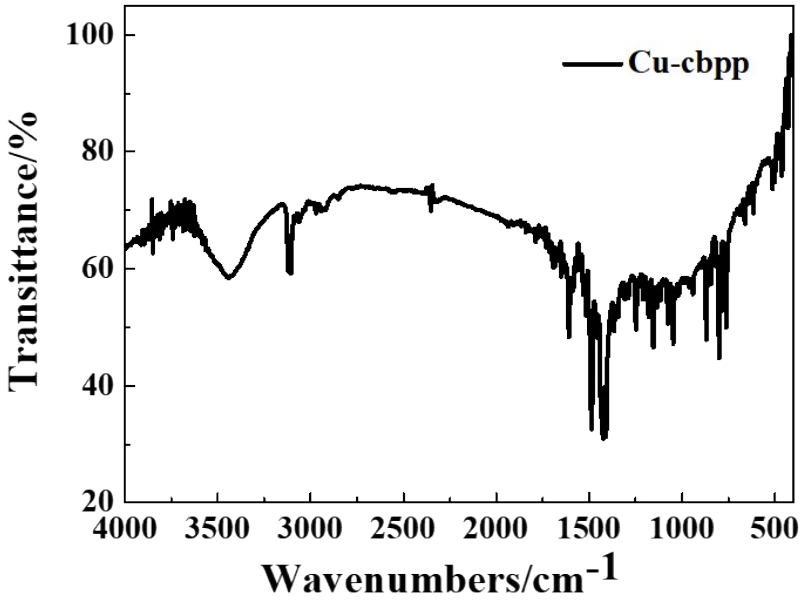


**Fig. S13** FT-IR spectra of Cu-cbpp

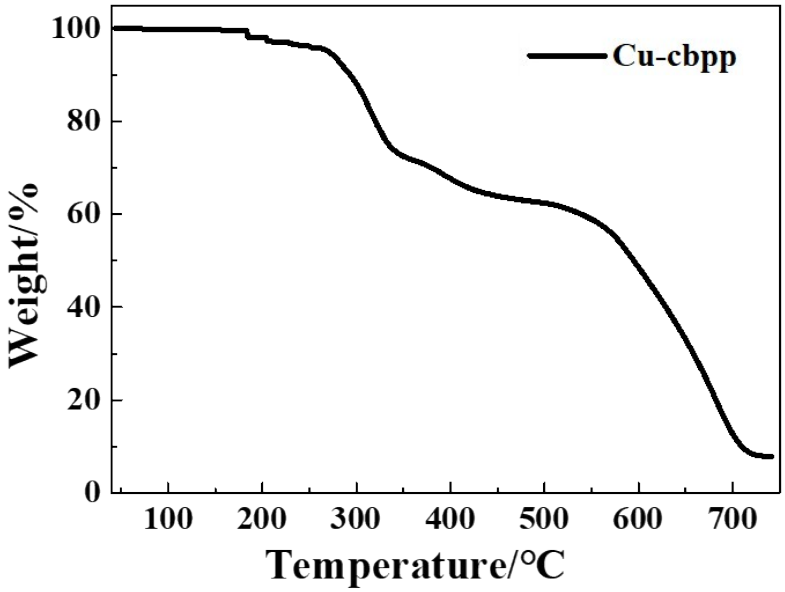


**Fig. S14** Thermal gravimetric curves of Cu-cbpp

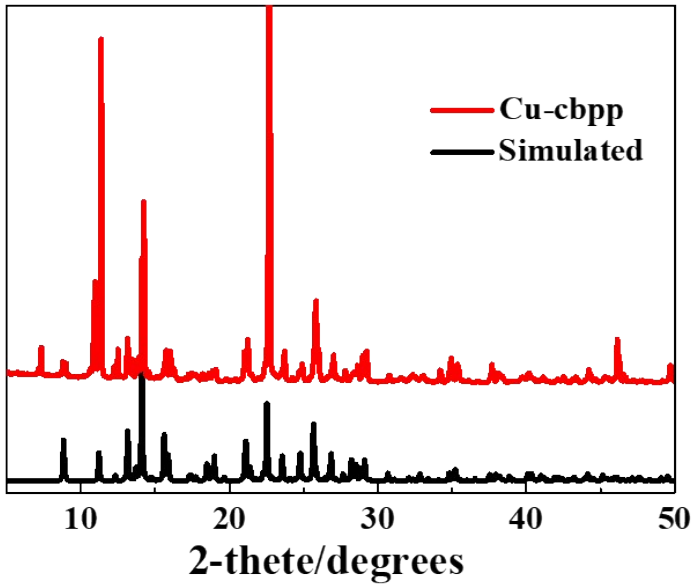


**Fig. S15** PXRD patterns of Cu-cbpp

**Table S3** Lifetime of Tb@Cu-Hcbpp in different urine chemicals

| Samples | Lifetime (μs) |
|---|---|
| Tb@Cu-Hcbpp | 194.74 |
| Tb@Cu-Hcbpp with NMF | 399.61 |
| Tb@Cu-Hcbpp with urea | 196.19 |
| Tb@Cu-Hcbpp with uric acid (UA) | 195.66 |
| Tb@Cu-Hcbpp with creatine | 192.53 |
| Tb@Cu-Hcbpp with creatinine (Cre) | 195.36 |
| Tb@Cu-Hcbpp with glucose (Glu) | 193.17 |
| Tb@Cu-Hcbpp with NaCl | 194.23 |
| Tb@Cu-Hcbpp with KCl | 194.65 |
| Tb@Cu-Hcbpp with $NH_4Cl$ | 195.01 |
| Tb@Cu-Hcbpp with $Na_3PO_4$ | 191.29 |

**Table S4** Standard deviation calculation

| No. | Fluorescence intensity ($I_{386}$) | Fluorescence intensity ($I_{544}$) | $I_{544}/I_{386}$ |
|---|---|---|---|
| 1 | 347.60 a.u. | 380.37 a.u. | 1.094275 |
| 2 | 345.47 a.u. | 379.37 a.u. | 1.098127 |
| 3 | 346.50 a.u. | 379.95 a.u. | 1.096536 |
| 4 | 345.41 a.u. | 379.48 a.u. | 1.098636 |
| 5 | 347.15 a.u. | 380.23 a.u. | 1.095290 |
| Average Value | -- | -- | 1.096573 |
| Standard Deviation (σ) | -- | -- | 0.000595 |
| Slope (*S*) for NMF | -- | -- | 0.08 $\mu M^{-1}$ |
| Detection limit (3σ/S) for NMF | -- | -- | 0.02 μM |
| Slope (*S*) for MGO | -- | -- | 0.0072$\mu M^{-1}$ |
| Detection limit (3σ/S) for MGO | -- | -- | 0.25μM |

**Table S5** Selected materials for sensing NMF

| No. | Complexes | Detection limit | References |
|---|---|---|---|
| 1 | Eu(III)@MOF-1 | 0.36 μM | *Sens. Actuators, B* 2018, 261, 153[1] |
| 2 | $[Eu_{0.1}Tb_{1.9}(FDA)_3(DMF)_2]\cdot 2DMF$ | -- | *Inorg. Chem. Front.* 2018, 5, 2971[2] |
| 3 | **Tb@Cu-Hcbpp** | **0.02 μM** | **This work** |

**Table S6** Selected materials for sensing MGO

| No. | Complexes | Detection limit | References |
|---|---|---|---|
| 1 | Methyl diaminobenzene-BODIPY or MBo | -- | *J. Am. Chem. Soc.* 2013, 135, 12429.[3] |
| 2 | Zr-UiO-66-$N_3$ | 118 μM | *Anal. Chem.* 2015, *87*, 1757.[4] |
| 3 | PDN-1 | 77 nM | *Anal. Methods* 2015, *7*, 2386.[5] |
| 4 | Pt/$CeO_2$/GLO | 2.14 nM | *Anal. Methods* 2016, *8*, 2207.[6] |
| 5 | L | -- | *Dyes Pigm.* 2017, *138*, 23.[7] |
| 6 | $V_2O_5$ modified electrode | 0.24 μM | *Biosens. Bioelectron.* 2018, *103*, 143.[8] |
| 7 | CMFP | 0.5 μM | *Anal. Chem.* 2019, *91*, 5646.[9] |
| 8 | **$Tb_{0.85}Yb_{0.15}$@Cu-Hcbpp** | **0.25 μM** | **This work** |

**Table S7** Lifetime of $Tb_{0.85}Yb_{0.15}$@Cu-Hcbpp in different serum chemicals

| Samples | Lifetime (μs) |
|---|---|
| $Tb_{0.85}Yb_{0.15}$@Cu-Hcbpp | 477.59 |
| $Tb_{0.85}Yb_{0.15}$@Cu-Hcbpp with MGO | 223.13 |
| $Tb_{0.85}Yb_{0.15}$@Cu-Hcbpp with PA | 485.63 |
| $Tb_{0.85}Yb_{0.15}$@Cu-Hcbpp with LA | 472.38 |
| $Tb_{0.85}Yb_{0.15}$@Cu-Hcbpp with AA | 473.42 |
| $Tb_{0.85}Yb_{0.15}$@Cu-Hcbpp with Cys | 475.94 |
| $Tb_{0.85}Yb_{0.15}$@Cu-Hcbpp with Ala | 475.33 |
| $Tb_{0.85}Yb_{0.15}$@Cu-Hcbpp with Glu | 473.53 |
| $Tb_{0.85}Yb_{0.15}$@Cu-Hcbpp with UA | 475.98 |
| $Tb_{0.85}Yb_{0.15}$@Cu-Hcbpp with NaCl | 477.19 |
| $Tb_{0.85}Yb_{0.15}$@Cu-Hcbpp with KCl | 476.73 |

## Note and references


1. N. Sun and B. Yan, *Sens. Actuators, B*, 2018, **261**, 153-160.
2. S.-J. Qin, X.-L. Qu and B. Yan, *Inorg. Chem. Front.*, 2018, **5**, 2971-2977.
3. T. Wang, E. F. Douglass, Jr., K. J. Fitzgerald and D. A. Spiegel, *J. Am. Chem. Soc.*, 2013, **135**, 12429-12433.
4. M. Havlikova, M. Zatloukalova, J. Ulrichova, P. Dobes and J. Vacek, *Anal. Chem.*, 2015, **87**, 1757-1763.
5. T. Tang, Y. Zhou, Y. Chen, M. Li, Y. Feng, C. Wang, S. Wang and X. Zhou, *Anal. Methods*, 2015, **7**, 2386-2390.
6. B. L. Ramachandra, S. Vedantham, U. M. Krishnan, N. Nesakumarabc, J. B. Balaguru and J. B. B. Rayappan, *Anal. Methods*, 2016, **8**, 2207-2217.
7. C. Liu, X. Jiao, S. He, L. Zhao and X. Zeng, *Dyes Pigm.*, 2017, **138**, 23-29.
8. L. Ramachandra Bhat, S. Vedantham, U. M. Krishnan and J. B. B. Rayappan, *Biosens. Bioelectron.*, 2018, **103**, 143-150.
9. H. Wang, Y. Xu, L. Rao, C. Yang, H. Yuan, T. Gao, X. Chen, H. Sun, M. Xian and C. Liu, *Anal. Chem.*, 2019, **91**, 5646-5653.